Egypt. J. Chem. Vol. 67, SI: M. R. Mahran, pp. **1167 - 1176** (2024)

Egyptian Journal of Chemistry

http://ejchem.journals.ekb.eg/

Elimination of Inorganic Pollutants Using a Novel Biomaterial Adsorbent

Fatiha Belalia[a,b], Alya Harichane [a], D. Belfennache[c], R. Yekhlef [c], S. Zaiou [d,e], Mohamed Hemdan [f], Mohamed A. Ali [f]

[a]*Institute of Science. Morsli Abdullah University Center- Tipaza 42000, Algeria.*
[b]*Treatments and Shaping Fibrous Polymers Laboratory (LTMFP). University of Boumerdes, Algeria..*
[c]*Research Center in Industrial Technologies CRTI, P.O. Box 64, Cheraga, 16014 Algiers, Algeria*
[d]*Laboratory for Studies of Surfaces and Interfaces of Solid Materials (LESIMS), University Setif 1, 19000 Setif, Algeria*
[e]*Faculty of Natural Sciences and Life, Setif-1 University, 19000 Setif, Algeria*
[f]*School of Biotechnology, Badr University in Cairo (BUC), Badr City 11829, Cairo, Egypt*

Abstract

This study examines the effectiveness of calcium alginate-carboxymethyl cellulose gel beads (Ca-A/CMC) as an innovative biomaterial for chromium ion (Cr^{3+}) adsorption. The composite hydrogel was created by physically cross-linking sodium alginate and carboxymethyl cellulose polymers in the presence of calcium ions. Various characterization techniques, including Fourier transform infrared (FTIR) spectroscopy and scanning electron microscopy (SEM), were used to analyze this novel biosorbent. These gel beads exhibit a significant adsorption capacity of 269.33 mg/g and a removal efficiency of 95%.The influence of different parameters, such as pH and contact time, on the adsorption capacity of Ca-A/CMC gel beads was investigated. The maximum adsorption capacity was achieved at a contact time of 120 minutes and a pH of 5.8. To understand the adsorption behavior, several kinetic and isothermal models were applied. The adsorption data were best described by the Langmuir isotherm model, with an R^2 value of 0.988, and the pseudo-second-order kinetic model, with an R^2 value of 0.9998. Thermodynamic analysis indicated that the adsorption process is spontaneous and endothermic. These findings demonstrate the high efficacy and potential application of Ca-A/CMC gel beads for removing Cr^{3+} ions in wastewater treatment.

Keywords: Chromium(III) adsorption; Alginate; Carboxymethyl cellulose; Wastewater treatment.

1. Introduction

Water pollution, particularly with toxic metals, remains a significant threat to both the natural environment and human health [1-3]. According to the World Health Organization (WHO), heavy metals in water sources can cause severe health problems, including neurological disorders and cancer. Globally, industrial processes contribute significantly to heavy metal pollution. For instance, the tanning industry alone produces approximately 40 million liters of wastewater containing chromium annually [4]. Chromium, a highly toxic and carcinogenic metal, is one of the most common pollutants in industrial effluents.

Chromium pollution in water is especially concerning due to its mutagenic and carcinogenic effects on biological species [5]. Widely used in industries such as electroplating, leather tanning, ceramics, pigment manufacturing, wood preservation, and paper production, chromium compounds generate substantial amounts of hazardous waste [6, 7]. In the environment, chromium exists in different oxidation states: Cr(0), Cr(III), and the highly toxic Cr(VI) [8]. Cr(VI) is particularly dangerous due to its high solubility, mobility in soil and water, and ability to permeate biological membranes [9, 10].

Various methods are employed to remove toxic metal ions, including chromium, from wastewater. These methods include adsorption, ion exchange, membrane separation, coagulation, chemical precipitation, extraction, dialysis, and electrochemical separation [11, 12]. Among these, adsorption stands out as the most environmentally friendly, economically viable, and technologically efficient technique. Modern adsorption

*Corresponding author e-mail: mohamed.ahmed_ali@buc.edu.eg; (Mohamed A. Ali).
Receive Date: 31 March 2024, Revise Date: 03 June 2024, Accept Date: 03 July 2024
DOI: 10.21608/ejchem.2024.280399.9541

technologies often use polymeric-based matrices as adsorbents due to their economic and technical advantages [13]. Polysaccharide-based bio-sorbents, such as alginate and carboxymethyl cellulose (CMC), are particularly effective due to their binding sites for divalent cations [14-16].

Calcium alginate/carboxymethyl cellulose (Ca-A/CMC) gel beads have shown promise in environmental applications, especially for adsorbing heavy metals and dyes from wastewater [17,18]. These beads leverage chemical, physical, and electrostatic mechanisms to achieve high removal rates of contaminants. They can be regenerated and reused multiple times, enhancing their sustainability. The combination of Ca-A and CMC improves the structural integrity and adsorption efficiency of the beads, making them highly effective for environmental remediation [18,19].

Our main goal is to optimize alginate's properties for effective water depollution and to study the efficacy of these materials. This work focuses on developing a protocol that ensures reproducibility and effectiveness of the beads, as well as a high adsorption rate. We aim to synthesize novel bio-sorbents from carboxymethyl cellulose (CMC) and sodium alginate (SA) for removing toxic metals, particularly chromium (III) ions, from wastewater. We synthesized cross-linked Ca-A/CMC gel beads and characterized them using FTIR and SEM. Adsorption tests were conducted to evaluate the impact of chromium ion concentration and adsorption duration on the beads' adsorption capacity. Finally, kinetic studies were performed to describe the adsorption process.

2. Materials and methods

2.1. Materials used for preparation of biopolymeric beads

For the synthesis of biopolymeric beads, widely available synthetic chemicals were utilized. Carboxymethyl cellulose (CMC), with a degree of substitution (DS) of 0.52 and a medium viscosity of 100 $Kg.mol^{-1}$, was obtained from Panreac. Sodium alginate (SA) was sourced from Labosi. Hydrated calcium chloride ($CaCl_2.2H_2O$) was purchased from Fluka. Chromium solutions, serving as the source of Cr (III) ions, were prepared from hydrated chromium chloride ($CrCl_3.6H_2O$). Only analytical grade reagents were used in the experiments. All aqueous solutions were prepared using distilled water.

2.2. Production of Ca-A-CMC gel beads

To prepare the biopolymeric beads, 2 grams of sodium alginate (SA) were dissolved in 100 mL of distilled water. This solution was stirred with a mechanical stirrer at 20°C until it became viscous. Then, 1.0 gram of carboxymethyl cellulose (CMC) was added to the SA solution, and the mixture was vigorously stirred for three hours. The resulting suspension was added dropwise into a calcium bath (500 mL) containing 0.05 mol/L calcium chloride solution at a regulated speed using a syringe [20]. This controlled rate prevents the sedimentation of coagulating Ca-A/CMC particles during bead formation. The optimal drop height for forming spherical beads was determined to be 6 cm. The beads were left to cure in the calcium bath overnight, allowing sufficient time for the gelation reaction to complete throughout the entire bead volume [21]. The coagulated beads were then repeatedly rinsed with distilled water to remove as much free calcium as possible. Subsequently, the biopolymeric particles were dried at 45°C in a lime kiln overnight until a constant mass was achieved [22, 23]. Finally, the dried beads were stored in desiccators until they were used in the adsorption experiments.

2.3. Characterization methods

The infrared spectra of the adsorbents before and after modification were recorded by a thermonicolet type FTIR spectrophotometer available at the Contonine-1 University. We carried out morphological observations using a TESCAN brand scanning electron microscope (SEM). (HITACHI S-4500, Acc Spot Magn 7.00 KV. Algeria). This device allows you to visualize the morphology and grain size of the samples. The images were taken in secondary electrons.

2.4. Cr (III) solution preparation

$CrCl_3.6H_2O$ was dissolved in double-distilled water to form a stock chromium solution with a concentration of 500 mg/l. This solution was then diluted using distilled water to prepare operational solutions with different concentrations of chromium required for the adsorption experiment.

2.5. Batch adsorption studies

Adsorption experiments of Cr(III) ions onto the previously prepared sorbent, namely biopolymeric Ca-A/CMC beads, followed the contact method outlined in [24]. Briefly, 0.1 g of beads were placed into a laboratory glass containing 50 ml of chromium (III) chloride solution to create the testing samples. To achieve the desired adsorption equilibrium, the mixture was kept at room temperature for 240 minutes in a temperature-controlled shaker with regular stirring at a speed of 250 rpm, maintaining a pH value of 5.8. Subsequently, samples were withdrawn from the shaker, the adsorbent was filtered, and the supernatant was centrifuged for 5 minutes to ensure homogeneity. The concentration of Cr (III) ions in the supernatant, representing the equilibrium concentration, was then quantified using atomic absorption spectrometry (AAS) (Zeenit 700 model Win AAS). The adsorption capacity (qe) and percentage removal (E) of metal ions from the solution in the performed experiment were expressed as equations (1) and (2), respectively.

$$q_t = (C_0 - C_e)V_0/m \quad (1)$$

$$E = (C_0 - C_e) \times 100/C_0 \quad (2)$$

Where: V_0 represents volume (l) of Cr (III) solution, C_0 and C_e are, respectively, initial and equilibrium concentrations (mg/l) of Cr (III) in solution, while *m* is weight of swollen spheres [23].

2.5.1. Study of adsorption kinetics

Three kinetic models were evaluated for the interpretation of data derived from batch studies to explore the adsorption kinetics mechanism: the pseudo-first-order model, the pseudo-second-order model, and the intraparticle diffusion model. The three kinetic models can be expressed by equations (3), (4), and (5), representing the pseudo-first-order, pseudo-second-order, and intraparticle diffusion models, respectively:

$$\log(q_e - q_t) = \log q_e - \frac{K_1}{2.303} t \quad (3)$$

$$\frac{t}{q_t} = \frac{t}{q_e} - \frac{1}{K_2 q_e^2} \quad (4)$$

$$q_t = K_{id} t^{1/2} + C \quad (5)$$

Where; K_1 and K_2 are the first-order and second-order rate constants (min^{-1}), respectively, and q_e and q_t represent adsorption quantities at equilibrium and at the time t ($mg.g^{-1}$). The intercept and slope of t/q_t vs. t linear plot are used to calculate K_2 and q_e, with q_e equal to 1/slope and K_2similar to slope^2/intercept. K_{id} is intra particular diffusion rate constant, q_t represents adsorption capacity at time t.

2.5.2. Adsorption isothermal models

Two adsorption isotherm models were utilized to investigate the adsorption process of Cr(III) using Ca-A/CMC gel beads: the Langmuir and Freundlich isotherm models. According to the Langmuir adsorption isotherm hypothesis, monolayer sorption occurs on a homogeneous surface of the adsorbent with identical adsorbing sites [25]. The relationship between the adsorption capacity of the beads and the concentration of chromium in the tested solution is represented by the Langmuir isotherm equations (6), (7), and (8), presented as follows:

$$q_e = 1 \frac{K_L C_e}{1 + K_L C_e} \quad (6)$$

The linearization of this function by taking the inverses gives:

$$\frac{1}{q_e} = \left(\frac{1}{K_L \times q_{max}}\right)\left(\frac{1}{C_e}\right) + \frac{1}{q_{max}} \quad (7)$$

This can also be expressed as:

$$C_e/q_e = 1/K_L . q_{max} + C_e/q_{max} \quad (8)$$

Where q_e represents the solute adsorbed in milligrams per gram of adsorbent, C_e is the solute's equilibrium concentration in the bulk solution (mg/L), K_L is the Langmuir constant (L/mg), and C_0 refers to the initial concentration of the ion. The separation factor R_L indicates the shape of the isotherm: it is characterized as irreversible if R_L=0, favorable if $0<R_L<1$, or unfavorable if $R_L>1$ [23].

The Freundlich adsorption isotherm can be represented by the following equations (10) and (11) respectively.

$$q_e = K_F C_e^{(1/n)} \quad (10)$$

$$log\ q_e = log\ K_F + \frac{1}{n} log\ C_e \quad (11)$$

Where: K_F is constant that indicates the relative adsorption capacity (mg/g), C_e is the equilibrium concentration of solute in the bulk solution (mg/L), and 1/n is a constant which shows intensity of adsorption process as well as the distribution of active sites. As an alternative, it is demonstrated through mathematical computation that n values ranging from 1 to 10 indicate advantageous adsorption [26]. It is also observed that the Freundlich isotherm is mathematically equivalent to the Langmuir isotherm under the condition where q_{max} approaches infinity or $K_L \ll 1$. In this context, the K_F value from the Freundlich equation corresponds to the K_L value from the Langmuir isotherm.

3. Results and discussion

3.1 FTIR analysis

The FTIR spectra of the alginate-carboxymethyl cellulose (Ca-A/CMC) gel beads before and after the adsorption of Cr(III) ions reveal significant changes in the intensities of characteristic peaks, providing valuable insights into the adsorption mechanism and the interactions between Cr(III) ions and the gel beads (Fig.1). Prior to adsorption, the FTIR spectrum of the Ca-A/CMC gel beads displays several prominent peaks: a broad peak around 3300 cm^{-1} corresponding to O-H stretching vibrations, indicative of hydroxyl groups present in both alginate and carboxymethyl cellulose; a peak around 2893 cm^{-1} attributable to C-H stretching vibrations; a strong peak at 1600 cm^{-1} due to asymmetric stretching of carboxylate groups (COO-) in alginate; a peak around 1419 cm^{-1} corresponding to symmetric stretching of carboxylate groups; and a peak near 1030 cm^{-1} indicative of C-O-C stretching vibrations, typical of glycosidic linkages in polysaccharides [27-29].

After the adsorption of Cr(III) ions, several factors contribute to the observed increase in intensity of FTIR bands. Firstly, there's an indication of enhanced binding affinity between Cr(III) ions and functional groups within the gel beads, potentially due to the formation of stronger chemical bonds like coordination complexes or chelates. Additionally, adsorption-induced conformational changes in the gel matrix may better align or expose functional groups to Cr(III) ions, increasing their participation in interactions. Moreover, the adsorption process could induce aggregation or clustering of functional groups, enhancing their collective contribution to FTIR signals. This aggregation may foster cooperative interactions between neighboring functional groups, intensifying vibrational modes. Furthermore, increased surface coverage of active sites by densely packed Cr(III) ions amplifies their contribution to FTIR signals. Synergistic effects and reduced vibrational damping also play roles, wherein interactions between Cr(III) ions and multiple functional groups occur simultaneously, leading to cooperative binding and reduced attenuation of vibrational modes, respectively. Lastly, the adsorption of Cr(III) ions might enhance the sensitivity of the FTIR technique to detect subtle vibrational changes within

the gel matrix, further accentuating band intensities [17,18].

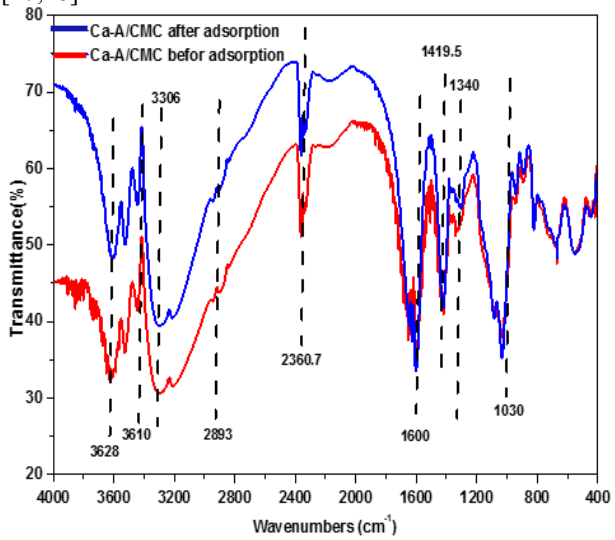

Fig.1. FTIR spectra of Ca-A/CMC gel beads before and after the adsorption of Cr(III) ions.

3.2. EM analysis

Understanding the structural changes in calcium alginate-carboxymethyl cellulose (Ca-A/CMC) gel beads before and after the adsorption process is essential for elucidating the interactions with Cr(III) ions (Fig.2). Initially, SEM images of the gel beads before adsorption exhibit a uniform and spherical morphology with a smooth surface, indicative of a well-formed gel matrix. Consistent particle size distribution and the presence of pores within the gel matrix highlight its porous nature, while interconnected networks of polymer chains suggest a cohesive and integrated structure [30,31].

Following adsorption, SEM images reveal notable modifications, including surface irregularities, roughness, and possible formation of new structures. Agglomeration of gel beads indicates interactions induced by Cr(III) ion adsorption, while changes in structural integrity, such as deformation or fragmentation, reflect the impact of the adsorption process. Additionally, alterations in pore morphology signify modifications in the internal structure of the gel beads induced by metal ion binding. Furthermore, the extent of surface coverage by Cr(III) ions is depicted, offering insights into adsorption sites and the distribution of metal ions on the gel bead surfaces [32].

3.3. Effect of different parameters on the adsorption process

The investigation into the adsorption process of Cr(III) ions using Ca-A/CMC gel beads concentrated on analyzing the influence of different parameters. Specifically, the study scrutinized the effects of contact time, initial concentration, and pH on the adsorption mechanism.

The contact time plays a crucial role in the efficiency of the adsorption process. In the investigation, the effect of contact time on the adsorption capacity and removal efficiency of the adsorbent was thoroughly examined (Fig.3a).

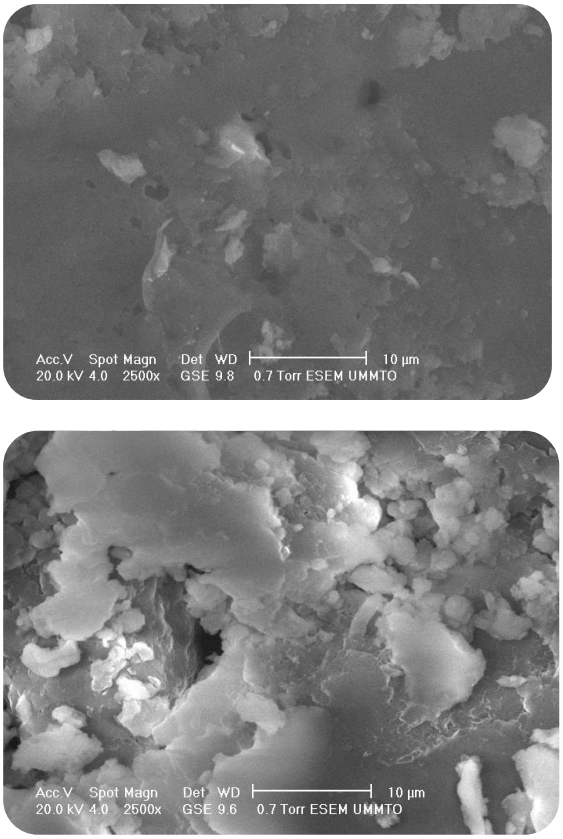

Fig.2. SEM images of: (a) Ca-A/CMC gel beads before adsorption and (b) after adsorption

It was observed that increasing the contact time from 20 minutes to 240 minutes resulted in a significant positive effect on both the adsorption capacity (q) and removal efficiency (E) of Cr(III) ions. Specifically, the adsorption capacity increased from approximately 220 mg/g to 232 mg/g, while the Cr uptake rose from around 88% to 92% within this timeframe. This observed trend can be attributed to the prolonged exposure duration, allowing for enhanced diffusion and interaction of Cr(III) ions with the available adsorption sites on the adsorbent surface. However, beyond 170 minutes, the graph depicting adsorption capacity and removal efficiency reaches a plateau, indicating saturation of adsorption sites. At this point, further contact time has minimal impact on Cr(III) removal, as all available locations on the adsorbent are occupied by Cr(III) ions [9, 33] .

The investigation delving into the impact of initial chromium ion concentration on the adsorption process highlighted significant correlations between the concentration of chromium ions in solution, spanning from 100 to 500 mg/l, and both the total adsorption capacity and percentage uptake by the Ca-A/CMC adsorbent (Fig. 3b). Maintaining a consistent dosage of 0.1 g/l of solution, it was noted that higher initial concentrations of Cr(III) ions corresponded to

increased adsorption capacity, escalating from 24.4 to 229.1 mg/g as the initial concentration rose from 50 to 500 mg/l, aligning with prior studies by J. H. Chen on sodium alginate-based membranes for chromium ion removal [32]. However, the effectiveness of adsorption reached a plateau beyond 300 mg/l, indicating saturation of the adsorbent with Cr(III) ions and restricting further uptake despite increased concentration. This saturation phenomenon resulted in a decline in the percentage removal of chromium ions, indicating a disruption of adsorption equilibrium. The decrease in percentage removal or uptake efficiency with increasing initial concentration can be attributed to the limited availability of adsorption sites as the concentration of chromium ions rises. At higher initial concentrations, the adsorbent may become fully occupied with Cr(III) ions, leading to fewer vacant sites for additional ions to adsorb onto the surface, thus diminishing removal efficiency despite the overall increase in adsorption capacity. Furthermore, the internal network structure of Ca-A/CMC gel beads, characterized by increased porosity and specific surface area, contributed to enhanced chromium ion removal rates [34].

The pH of the solution plays a pivotal role in determining the efficacy of the adsorption process of Cr(III) using calcium alginate carboxymethyl cellulose gel beads (Fig .3c). As shown in the figure, varying pH levels distinctly impact the adsorption capacity of the beads. At lower pH values, such as pH 2.51 and 3.36, the adsorption capacity remains relatively low, measuring 10.03 mg/g and 11.74 mg/g respectively. However, a notable increase in adsorption capacity is observed with increasing pH. At pH 4.81, there's a significant surge in adsorption capacity, reaching 65.25 mg/g, indicating an optimal pH range for enhanced adsorption. This trend continues with further pH increments, peaking at pH 5.8 with an impressive adsorption capacity of 93.33 mg/g. Beyond this optimal pH, a slight decline in adsorption capacity is noted, albeit remaining relatively high. At pH 7.28, 8.51, and 11.32, the adsorption capacities are 88.02 mg/g, 79.74 mg/g, and 77.05 mg/g respectively. This comprehensive data underscores the critical influence of pH on maximizing the adsorption capacity of Cr(III) onto calcium alginate carboxymethyl cellulose gel beads, elucidating the importance of pH control in optimizing adsorption processes [31].

3.4. Adsorption kinetics

The adsorption kinetics of chromium (III) ions onto Ca-A/CMC gel beads were systematically studied. The mathematical expressions and kinetic parameters for the adsorption process of Cr(III) onto Ca-A/CMC gel beads are represented in Table1.

The pseudo-second-order model exhibited a higher R^2 value (0.9998) compared to the pseudo-first-order model (R^2=0.96) and the intra-particle diffusion model (R^2=0.929), indicating a better fit for the adsorption process. Therefore, the pseudo-second-order kinetic model was identified as the most appropriate for describing the adsorption of chromium (III) ions onto Ca-A/CMC gel beads. Fig. 4 illustrates the kinetic plots for the three investigated kinetic models .

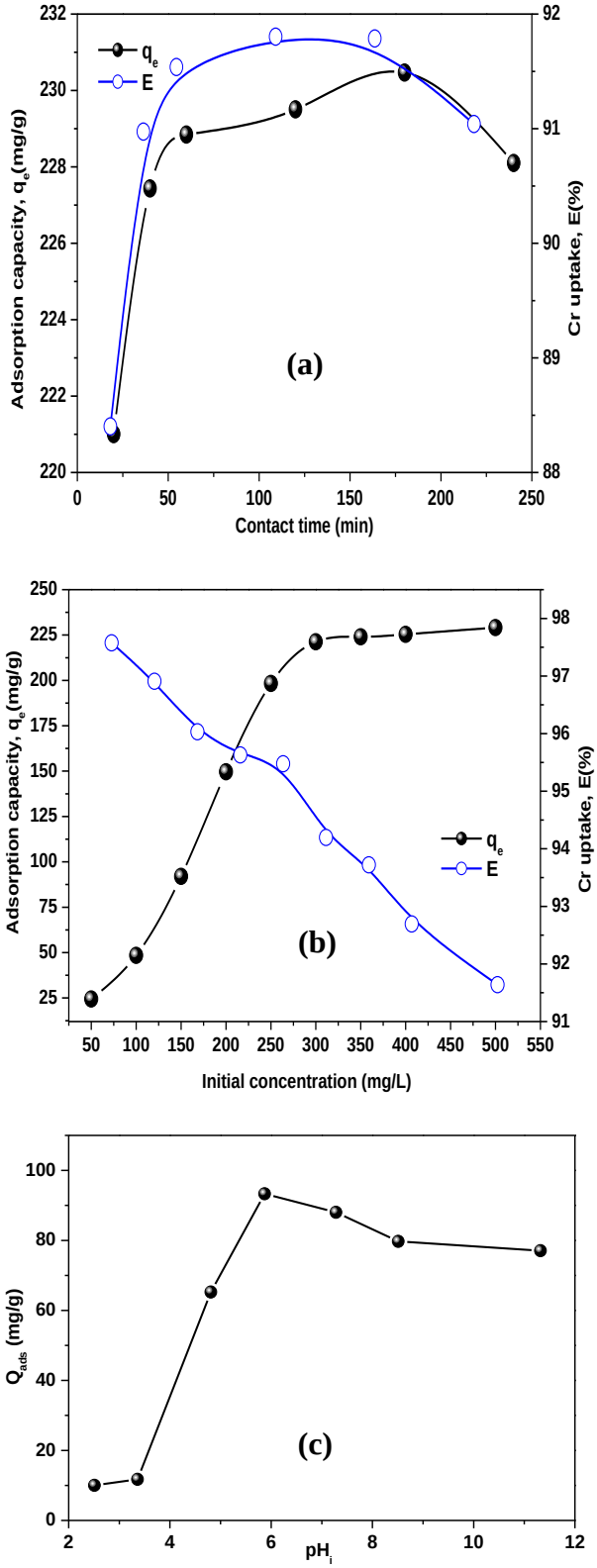

Fig.3. Examining the effect of various parameters on the adsorption process: (a) Contact time, (b) Initial concentration, and (c) pH.

Notably, the plots did not pass through the origin, suggesting that the adsorption process was complex and dominated by extra-particle diffusion rather than intra-particle diffusion. This implies a multistep-limited adsorption process for chromium ions in this study. Initially, chromium ions diffuse through the outer layer onto the Ca-A/CMC network structure, involving interactions between hydroxyl groups in CMC and carboxyl groups in SA. In the subsequent phase (t=120 min), ions are gradually adsorbed onto the adsorbent, slowing down intra-particle diffusion due to the decreased ion concentration in the solution [32-38].

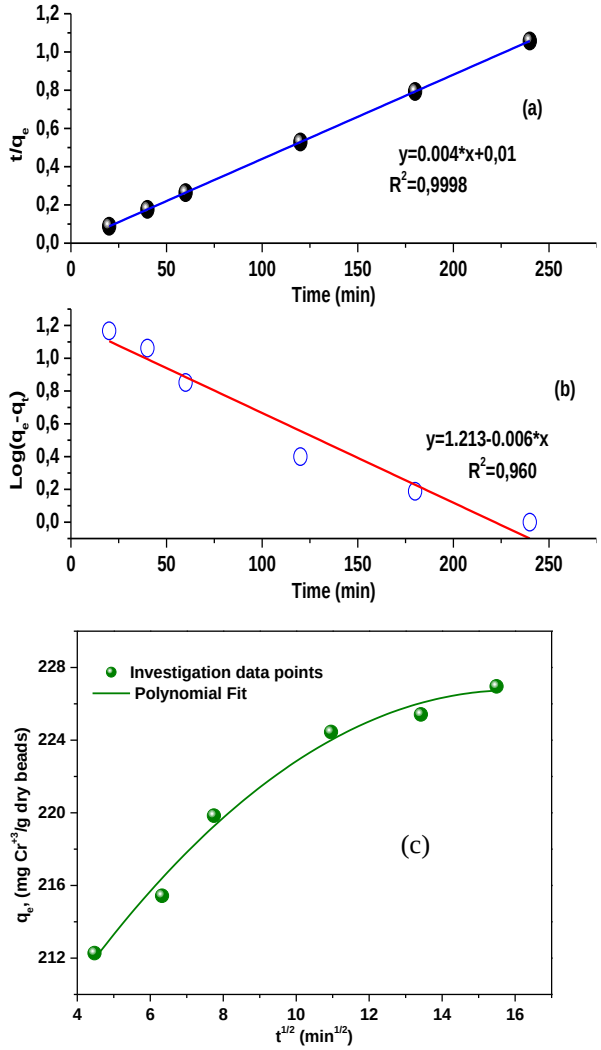

Fig.4. Kinetic Plots for the Adsorption of Chromium (III) Ions onto Ca-A/CMC Gel Beads: (a) Pseudo-Second-Order Model, (b) Pseudo-First-Order Model, (c) Intra-Particle Diffusion Model.

3.5. Adsorption isotherms and thermodynamics

In our detailed investigation into the adsorption behavior of Cr(III) ions onto Ca-A/CMC gel beads, we rigorously evaluated several isotherm models to elucidate the underlying dynamics of this process. Among the models examined, the Langmuir and Freundlich isotherm models were employed to capture the intricate interactions involved in Cr(III) adsorption (Figs. 5 and 6). The calculated parameters for these models are presented in Table 2, providing a comprehensive understanding of the adsorption mechanisms at play.

The adsorption data revealed a clear trend: the amount of adsorbed chromium ions increased with the concentration of chromium ions in the solution, eventually reaching a saturation point. This plateau indicates that the adsorption sites on the Ca-A/CMC gel beads became fully occupied, signifying the maximum adsorption capacity had been achieved [20]. For the Langmuir isotherm model, the calculated parameters include an adsorption capacity (q_{max}) of 269.33 mg/g, a Langmuir constant (K_L) of 0.120 L/mg, and a correlation coefficient (R^2) of 0.988. Additionally, the separation factor (R_L) ranged from 0.256 to 0.033, suggesting a strong affinity between Cr(III) ions and the adsorption sites, and indicating efficient adsorption across various initial concentrations.

Conversely, the Freundlich isotherm model parameters for Ca-A/CMC gel beads were determined as follows: a Freundlich constant (K_F) of 0.0895, a Freundlich exponent (n) of 1.281, and a value of 1/n at 0.780, which falls within the range of $0 < n < 10$. The value of n greater than 1 suggests a favorable adsorption process, implying that bond energies increase with surface density. The 1/n value of less than 1 further supports this favorability, indicating a heterogeneous surface with a non-uniform distribution of adsorption heat. A comparative analysis of the models revealed that the Langmuir isotherm model, with its higher correlation coefficient ($R^2 > 0.988$), provided a more accurate representation of the adsorption process than the Freundlich isotherm model ($R^2 < 0.923$). The Langmuir model's assumption of monolayer adsorption on a homogeneous surface aligns well with the experimental results, suggesting that the adsorption sites on the Ca-A/CMC gel beads are uniform and equivalent [31].

In the investigation of different thermodynamic parameters and depending on previously published studies utilizing the same adsorbent materials, calcium alginate and carboxymethyl cellulose (Ca-A/CMC gel), for the adsorption of similar ions such as Cr(III) under comparable conditions and adsorption mechanisms, several key observations were made. The process exhibited spontaneity and feasibility, evident from negative Gibbs free energy (ΔG°) values. Remarkably, as temperature rose, ΔG° became more negative, suggesting heightened spontaneity. Additionally, the positive enthalpy change (ΔH°) indicated an endothermic process, implying enhanced adsorption efficiency at higher temperatures. Furthermore, the positive entropy change (ΔS°) hinted at increased randomness during adsorption [16-20].

Table 1: Kinetic parameters of pseudo-first order, pseudo-second order, and intra particle diffusion models for adsorption of Cr(III) onto Ca-A/CMC beads

Pseudo-first-order		**Pseudo-second-order**		**Intra particle diffusion model**	
q_e(mg/g)	16.33	**q_e (mg/g)**	250	**C (mg/g)**	207.74
K_1(g/mg.min)	0.0115	**K_2 (g/mg.min)**	0.0016	**K_{id} (mg/g.min$^{1/2}$)**	1.333
R^2	0.96	**R^2**	0.9998	**R^2**	0.929

Table 2: The isothermal parameters of Freundlich and Langmuir models.

Langmuir Model	
Adsorption capacity; q_{max}(mg/g)	269.33
Langmuir constant; K_L (L/mg)	0.120
Correlation coefficient; R^2	0.988
Separation factor: R_L	0.256÷ 0.033
Freundlich Model	
Freundlich constant; n	1.281
Predicted sorption; K_F (mg/g(L/mg)$^{1/n}$)	0.0895
Correlation coefficient; R^2	0.923
Standard free energy: ΔG_0 (KJ/ mol) at 299K	-2.235
Adsorption type	Physical type

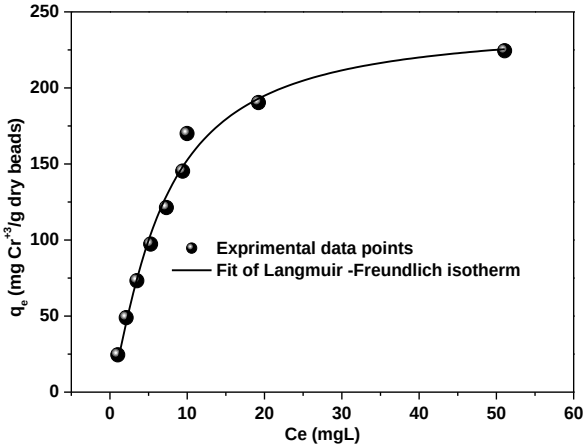

Fig. 5. Experimental data points for Langmuir and Freundlich isotherm models for Cr(III) adsorption onto Ca-A/CMC gel beads.

3.6. Comparison with other Cr(III) adsorbents

As seen in Table 3, the adsorption capacity of calcium alginate carboxymethyl cellulose (Ca-A/CMC) gel beads for Cr(III) was evaluated and compared with several other adsorbents. The Ca-A/CMC gel beads demonstrated a remarkable sorption capacity of 269.33 mg/g for trivalent chromium ions with a contact time of 240 minutes, as observed in the present study. This performance is significantly higher than that of other reported adsorbents. For instance, sodium alginate-based porous membranes achieved a sorption capacity of 57.4 mg/g within the same contact time [32]. Alumina nanoparticles immobilized on zeolite exhibited a notably lower sorption capacity of 182 mg/g [38]. Modified lignin and bentonite clay also showed moderate adsorption capacities of 25 mg/g and 49.75 mg/g respectively, with the latter achieving this in a much shorter contact time of 15 minutes [39,40].

Activated alumina powder (AAP) was found to have a high sorption capacity of 121.19 mg/g, but it still falls short compared to the Ca-A/CMC gel beads [41]. Powdered wool, on the other hand, displayed a relatively low adsorption capacity of 23 mg/g [42]. These comparisons highlight the superior efficiency of Ca-A/CMC gel beads in adsorbing Cr(III), making them a highly effective material for removing trivalent chromium from aqueous solutions. The high adsorption capacity and the relatively reasonable contact time underscore the potential of Ca-A/CMC gel beads as a promising adsorbent for industrial applications in water treatment.

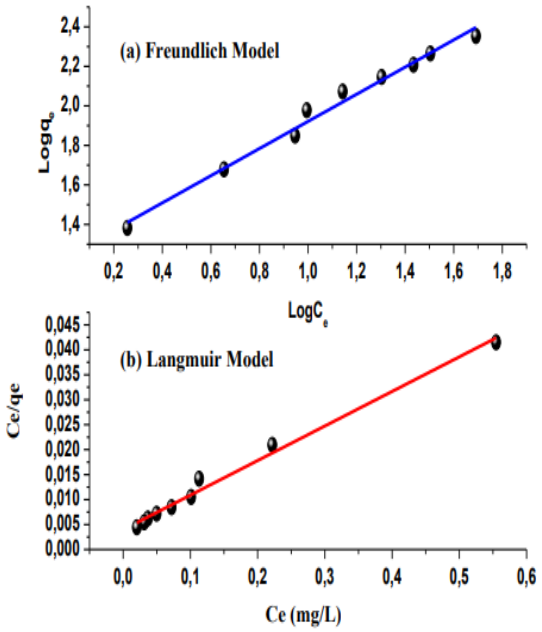

Fig.6. Isothermal plots for investigating the adsorption process of Cr(III) using Ca-A/CMC gel beads: (a) Freundlich model, and (b) Langmuir model.

Table 3: Diverse bio adsorbent utilized for chromium (III) metal ions.

Adsorbent	Chromium ion	Adsorption capacity ($mg.g^{-1}$)	Contact time (min)	Ref.
Sodium alginate-based porous membrane	Trivalent	57.4	240	[32]
Alumina nanoparticles immobilized zeolite	Trivalent	182	240	[38]
Modified Lignin	Trivalent	25	240	[39]
Bentonite clay	Trivalent	49.75	15	[40]
Activated alumina powder (AAP)	Trivalent	121.19	50	[41]
Powdered wool	Trivalent	23	180	[42]
Ca-A/CMC gel beads	Trivalent	269.33	120	This work

4. Conclusions

In conclusion, calcium alginate-carboxymethyl cellulose (Ca-A/CMC) gel beads exhibit remarkable potential as an efficient biomaterial for Cr^{3+} ion adsorption. The composite hydrogel, with an adsorption capacity of 269.33 mg/g and a removal efficiency of 95%, demonstrates promise for wastewater treatment. Optimal conditions were found at pH 5.8- and 120-minutes contact time, with Langmuir and pseudo-second-order kinetic models providing the best fit. Thermodynamic analysis confirms the process's spontaneity and endothermic nature. Beyond technical merits, this research highlights the broader implications for environmental protection and sustainable development. Ca-A/CMC gel beads contribute to advancing water purification, fostering cleaner environments. Future research could focus on optimization strategies and explore applications for removing other heavy metal ions and pollutants, thereby driving innovation in environmental stewardship.

5. References

[1] C. Zamora-Ledezma, D. Negrete-Bolagay, F. Figueroa, E. Zamora-Ledezma, M. Ni, F. Alexis, V.H. Guerrero. Heavy metal water pollution: A fresh look about hazards, novel and conventional remediation methods, Environ. Technol. Innov. 22 (2021) 101504. https://doi.org/10.1016/j.eti.2021.101504

[2] M.F. Mubarak, H. Selim, H.B. Hawash, M. Hemdan, Flexible, durable, and anti-fouling maghemite copper oxide nanocomposite-based membrane with ultra-high flux and efficiency for oil-in-water emulsions separation. Environ. Sci. Pollut. Res. 31 (2024)2297–2313. https://doi.org/10.1007/s11356-023-31240-x.

[3] A.K. El-Sawaf, M. Hemdan, H. Selim, A.A. Nassar, M.F. Mubarak, Revolutionizing water treatment: Enhanced flux and selectivity in polyethersulfone mixed matrix membrane through magnetic CuO-functionalized Fe3O4 nanoparticles for synthetic oily produced water remediation. Surfaces and Interfaces 46 (2024)104142. https://doi.org/10.1016/j.surfin.2024.104142.

[4] Ahmed E., Abdulla H. M.., Mohamed A. H., El-Bassuony A. D., Remediation and recycling of chromium from tannery wastewater using combined chemical–biological treatment system. Process Saf. Environ. Prot 2016. 104:1-10. https://doi.org/10.1016/j.psep.2016.08.004

[5] Costa, M., Klein, C. B., Toxicity and carcinogenicity of chromium compounds in humans. Crit. Rev. Toxicol, 2006. 36(2): 155-163. https://doi.org/10.1080/10408440500534032

[6] Jang E.-H., Pack, S. P., Kim I., Chung S., A systematic study of hexavalent chromium adsorption and removal from aqueous environments using chemically functionalized amorphous and mesoporous silica nanoparticles. Scientific reports, 2020. 10(1): 5558. https://doi.org/10.1038/s41598-020-61505-1

[7] Kumar H. Maurya K. L., Gehlaut A. K., D. Singh, Sanjeev Maken, Ankur Gaur, Suantak Kamsonlian., Adsorptive removal of chromium (VI) from aqueous solution using binary bio-polymeric beads made from bagasse. Appl. Water Sci., 2020. 10(1): 1-10. https://doi.org/10.1007/s13201-019-1101-y

[8] Pebdeni, A.B., Kudahi S.N., Hosseini M., Environmental applications of luminescent metal nanoclusters, Luminescent Metal Nanoclusters. 2022: 465-491. https://doi.org/10.1016/B978-0-323-88657-4.00011-9

[9] Kadam, A.N., Lee J., Nipane S. V., Lee S.W., Nanocomposites for visible light photocatalysis, Nanostructured Materials for Visible Light Photocatalysis, 2022: 295-317. https://doi.org/10.1016/B978-0-12-823018-3.00017-8

[10] Shukla, O. Rai U., Hexavalent chromium induced changes in growth and biochemical responses of chromate-resistant bacterial strains isolated from tannery effluent. Bull

Environ Contam Toxicol. 2006. 77(1). doi: 10.1007/s00128-006-1037-4.

[11] Shrestha, R., Ban S., Devkota S., Sharma S., Joshi R., Tiwari A.P., Kim H.Y., Joshi M.K., Technological trends in heavy metals removal from industrial wastewater: A review. J. Environ. Chem. Eng. 2021. 9(4): 105688. https://doi.org/10.1016/j.jece.2021.105688

[12] Saleh, T.A., Mustaqeem M., Khaled M., Developing water treatment technologies in removing heavy metal ions from wastewater: A review. Environ. Nanotechnol. Monit. Manag., 2021. 17:100617.
DOI: 10.1016/j.enmm.2021.100617

[13] Kandile, N.G. Nasr A.S., Environment friendly modified chitosan hydrogels as a matrix for adsorption of metal ions, synthesis and characterization. Carbohydr. Polym., 2009. 78(4):753-759. https://doi.org/10.1016/j.carbpol.2009.06.008

[14] Zhao, C., Liu G., Tan Q., Gao M., Chen G., Huang X., Xu X., Li L., Wang J., Zhang Y, Xu D., Polysaccharide-based biopolymer hydrogels for heavy metal detection and adsorption. J. Adv. Res., 2023. 44:53-70.
DOI: 10.1016/j.jare.2022.04.005

[15] Klein, M. Poverenov E., Natural biopolymer based hydrogels for use in food and agriculture. J. Sci. Food Agric., 2020. 100(6): 2337-2347.
DOI: 10.1002/jsfa.10274

[16] Salim, A.J., Adsorption of hexavalent chromium ion from aqueous solution by sodium alginate and carboxymethyl cellulose beads: kinetics and isotherm studies. Al-Nahrain Journal of Science, 2015. 18(4): 40-48.

[17] Yu, H. Li, H. Ma, L. Zhang, Y. Li, Q. Lin, Characteristics and mechanism of Cu(II) adsorption on prepared calcium alginate/carboxymethylcellulose@MnFe2O4. Polymer Bulletin. (2022) 79 : 1201–1216. https://doi.org/10.1007/s00289-021-03555-7

[18] J. Fu, J. X. Yap, C.P. Leo, C.K. Chang, Carboxymethyl cellulose/sodium alginate beads incorporated with calcium carbonate nanoparticles and bentonite for phosphate recovery. Int. J. Biol. Macromol. (2023) 234: 123642. https://doi.org/10.1016/j.ijbiomac.2023.123642

[19] W. Li, L. Zhang, D. Hu, R. Yang, J. Zhang, Y. Guan, F. Lv, H. Gao. A mesoporous nanocellulose/sodiumalginate/carboxymethyl -chitosan gel beads for efficient adsorption of Cu2+ and Pb2+, Int. J. Biol. Macromol. 187 (2021) 922–930.

[20] Tiwari A., Dewangan T., Bajpai A., Removal of toxic As (V) ions by adsorption onto alginate and carboxymethyl cellulose beads. J Chin Chem Soc-Taip., 2008. 55(5): 952-961. DOI: 10.1002/jccs.200800142

[21] Rocher V., Siaugue J-M., Cabuil V., Bee A., Removal of organic dyes by magnetic alginate beads. Water research, 2008. 42(4-5):1290-1298. https://doi.org/10.1016/j.watres.2007.09.024

[22] Belalia F., Djelali N.-E., Rheological properties of sodium alginate solutions. Rev. Roum. Chim, 2014. 59(2):135-145.

[23] Belalia, F. Djelali N.-E., Investigation of swelling/adsorption behavior of calcium alginate beads. Rev. Roum Chim, 2016. 61(10):747-754.

[24] Bajpai, A. Sachdeva R., Adsorption of casein onto alkali treated bentonite. J. Appl. Polym. Sci., 2000. 78(9): 1656-1663. https://doi.org/10.1002/10974628(20001128)78:9<1656:

[25] Langmuir I., The adsorption of gases on plane surfaces of glass, mica and platinum. J. Am. Chem. Soc., 1918. 40(9): 1361-1403. https://doi.org/10.1021/ja02242a004

[26] McKay G., Adsorption of dyestuffs from aqueous solutions with activated carbon I: Equilibrium and batch contact-time studies. J Chem Technol, 1982. 32(7-12): 759-772. https://doi.org/10.1002/jctb.5030320712

[27] Reed B.E. Matsumoto M.R., Modeling cadmium adsorption by activated carbon using the Langmuir and Freundlich isotherm expressions. SEP SCI TECHNOL, 1993. 28(13-14): 2179-2195. https://doi.org/10.1080/01496399308016742

[28] Dewangan, T., A. Tiwari, Bajpai A., Removal of chromium (VI) ions by adsorption onto binary biopolymeric beads of sodium alginate and carboxymethyl cellulose. J. Dispers. Sci. Technol, 2011. 32(8):1075-1082. https://doi.org/10.1080/01932691003659403

[29] Dewangan, T., Tiwari A., Bajpai A.K, Adsorption of Hg (II) ions onto binary biopolymeric beads of carboxymethyl cellulose and alginate. J. Dispers. Sci. Technol. 2010. 31(6): 844-851. https://doi.org/10.1080/01932690903212941

[30] Vunain, E., Njewa J.B, Timothy Tiwonge Biswick T.T., Ipadeola A.K., Adsorption of chromium ions from tannery effluents onto activated carbon prepared from rice husk and potato peel by H_3PO_4 activation. Appl. Water Sci., 2021. 11(9):150. https://doi.org/10.1007/s13201-021-01477-3

[31] A.H. Ragab, M.F. Mubarak, H.A. El-Sabban, J.H. Kang, A. El Shahawy, H.A. Alshwyeh, M. Hemdan. Exploring the sustainable synthesis pathway and comprehensive characterization of magnetic hybrid alumina nanoparticles phase (MHAl-NPsP) as highly

efficient adsorbents and selective copper ions removal, Environ. Technol. Innov. 34 (2024) 103628. https://doi.org/https://doi.org/10.1016/j.eti.2024.103628.

[32] Chen J.H., Preparation and investigation on the adsorption behavior of polyethylene glycol modified sodium alginate porous membrane adsorbent for Cr (III) ions. Adv. Mater. Res. 2012. 455:786-795. https://doi.org/10.4028/www.scientific.net/AMR.455-456.786

[33] Bajpai J., Shrivastava R. Bajpai A., Binary biopolymeric beads of alginate and gelatin as potential adsorbent for removal of toxic Ni^{2+} ions: a dynamic and equilibrium study. J. Appl. Polym. Sci., 2007. 103(4):2581-2590. DOI: 10.1002/app.25198

[34] M.A. Ali, M.F. Mubarak, M. Keshawy, M.A. Zayed, M. Ataalla, Adsorption of Tartrazine anionic dye by novel fixed bed Core-Shell-polystyrene Divinylbenzene/Magnetite nanocomposite, Alexandria Eng. J. 61 (2022) 1335–1352. https://doi.org/https://doi.org/10.1016/j.aej.2021.06.016.

[35] Manzoor Q., Sajid A., Hussain T., Iqbal M. Abbas A., Nisar J., Efficiency of immobilized Zea mays biomass for the adsorption of chromium from simulated media and tannery wastewater. Journal of Materials Research and Technology 8.1(2019): 75-86 https://doi.org/10.1016/j.jmrt.2017.05.016

[36] Sadiq A., Choubey A. Bajpai A., Biosorption of chromium ions by calcium alginate nanoparticles. J. Chil. Chem. Soc., 2018. 63(3):4077-4081. http://dx.doi.org/10.4067/s071797072018000304077.

[37] Yakun H. Ding W., Huang X., Xu J., Zhao M., Fluoride removal by lanthanum alginate bead: adsorbent characterization and adsorption mechanism. Chin. J. Chem. Eng. 2011. 19(3):365-370. https://doi.org/10.1016/S1004-9541(09)60222-6

[38] Deravanesiyan M., Beheshti M. Malekpour A., Alumina nanoparticles immobilization onto the NaX zeolite and the removal of Cr (III) and Co (II) ions from aqueous solutions. J. Ind. Eng. Chem., 2015. 21: 580-586. https://doi.org/10.1016/j.jiec.2014.03.023

[39] Demirbaş A., Adsorption of Cr (III) and Cr (VI) ions from aqueous solutions on to modified lignin. Energy Sources, 2005. 27(15): 1449-1455. https://doi.org/10.1080/009083190523352

[40] Tahir S., Naseem R., Removal of Cr (III) from tannery wastewater by adsorption onto bentonite clay. SEP PURIF TECHNOL, 2007. 53(3):312-321.https://doi.org/10.1016/j.seppur.2006.08.008

[41] Rajurkar N.S., Gokarn A.N., K. Dimya, Adsorption of chromium (III), nickel (II), and copper (II) from aqueous solution by activated alumina. Clean–Soil, Air, Water, 2011. 39(8): 767-773. https://doi.org/10.1002/clen.201000273

[42] N.J. Khengare, S.N. Labade, K.M. Lalge, V.S. Patil, C.J. Khilare, S.S. Sawant. Effective removal of chromium from aqueous solution by adsorption on powdered wool: In-silico studies of adsorption mechanism, Chem. Data Collect. 41 (2022) 100935. https://doi.org/https://doi.org/10.1016/j.cdc.2022.100935.